



## Identifying the apparent and true grinding limit

C. Knieke, M. Sommer<sup>1</sup>, W. Peukert<sup>\*</sup>

*Institute of Particle Technology, Friedrich-Alexander-University, Cauerstraße 4, 91058 Erlangen, Germany*

### ARTICLE INFO

#### Article history:

Received 19 September 2008  
Received in revised form 27 April 2009  
Accepted 7 May 2009  
Available online 20 May 2009

#### Keywords:

Ultrafine grinding  
Grinding limit  
Microstructure analysis  
Stirred media mill

### ABSTRACT

Comminution in stirred media mills enables the production of ultrafine particles down to the nanometer range. The grinding results are mainly determined by two contrary mechanisms: particle breakage and agglomeration of the so-created fragments. These competing phenomena often lead to a plateau in particle size above a certain energy input. The degree of agglomeration and therefore the final aggregate size can be controlled by the addition of stabilizers and by the applied shear forces. In this paper the agglomeration behavior of silica particles under different milling and stability conditions is presented. Furthermore the particle breakage behavior in the nanometer range as the other size-determining mechanism will be discussed. In long term grinding experiments with different materials the kinetics of particle breakage as well as the grinding limit as the minimal achievable particle size could be obtained.

© 2009 Elsevier B.V. All rights reserved.

### 1. Introduction

Nanoparticles are increasingly used in many areas of chemical and pharmaceutical as well as in ceramic and microelectronic industry. Besides the direct synthesis of these materials by chemical methods, wet grinding in stirred media mills is a suitable technique for the production of nanoparticles in the liquid phase with high solid concentrations [1–3]. The manufacturing of fine particles is influenced by particle breakage and interparticle interactions. The interactions become relevant especially for particles smaller than 1  $\mu\text{m}$  because of an increasing collision rate of the particles due to their Brownian motion [4]. In most grinding experiments a limit in particle size is reached where further energy input does apparently not lead to smaller particle sizes. Stenger et al. [1] demonstrated that this observed limit is dependent on the stability of the suspension. By means of electrostatic, steric or electrosteric stabilization and shear stress this so called apparent grinding limit can be shifted to smaller particle sizes. Whereas the apparent grinding limit can be controlled by the interparticle interactions, the true grinding progress only refers to the actual breakage of particles. The existence of this true grinding limit as the minimal achievable particle size in grinding experiments, where no further particle breakage occurs even after excessive energy input, is an essential question in nanogrinding. By means of X-ray diffraction analysis the evolution of internal microstructural features such as the crystallite size (coherent domain size) and the lattice strain can be examined to understand the breakage mechanism in the nanometer range.

Investigations in microstructural changes during comminution processes are already established in the field of mechanical alloying, where extremely fine microstructures of elementary metals or alloys can be produced by mechanical stressing in high-energy ball mills [5–7]. Alloying processes are realized as dry grinding processes commonly using planetary ball mills. There, different mechanisms concerning the particle breakage and the grinding limit of the metal alloy particles take place compared to ultrafine wet grinding of oxide particles in stirred media mills. Therefore, rather limited experience can be transferred from mechanical alloying to the grinding behavior of oxide particles stressed in stirred media mills. Nevertheless, Forsberg et al. investigated microstructural changes during grinding of hematite particles in different types of mills, among them a stirred media mill. By means of X-ray diffraction analysis the development of crystallite size and microstrain determined by different evaluation methods of the measured patterns were presented [8,9]. A so called steady state of the crystallite size at 11 nm determined by Rietveld analysis was observed in the stirred media mill after a specific energy input of 82,000 kJ/kg.

Further studies into the grinding limit in comminution processes were described by Koch [10], Karagedov and Lyakhov [11], Boldyrev et al. [12] and Cho et al. [13]. Koch and Karagedov investigated the minimum achievable grain size in dry grinding processes in planetary ball mills. Here the smallest crystallite size was attributed to a dynamic equilibrium between the mechanical splitting of crystallites and their coalescence by thermal processes. Eckert [14] found that the minimum grain sizes of the fcc metals in such dry grinding processes scale inversely with their melting temperatures. Boldyrev et al. described that a general grinding limit is equal to the size where ductile–brittle transition occurs. Below that size the relaxation mechanism is assumed to change from brittle fracture to ductile flow. Boldyrev refers to Schönert, who affirmed that stressed particles that are larger than a certain size experience breakage if the stress

<sup>\*</sup> Corresponding author. Tel.: +49 9131 8529400; fax: +49 9131 8529402.

E-mail address: [w.peukert@lfg.uni-erlangen.de](mailto:w.peukert@lfg.uni-erlangen.de) (W. Peukert).

<sup>1</sup> Currently affiliated to Infracerv GmbH & Co. Gendorf KG, Industriepark Werk Gendorf, 84504 Burgkirchen, Germany.

intensity is sufficient, while smaller particles undergo plastic deformation only [15]. In 1996 Cho et al. presented results from long term grinding experiments of crystalline quartz in a stirred media mill. A grinding limit of about 40 nm diameter was obtained under the applied milling conditions.

In this paper we present results of long term grinding experiments of different materials in a stirred media mill and discuss the influencing parameters on breakage kinetics and the grinding limit. With the knowledge about the breakage behavior in the nanometer range comminution processes in the field of wet ultrafine grinding can be controlled and optimized in order to avoid excessive energy input which in turn increases the efficiency of milling.

## 2. Experimental

### 2.1. Materials

#### 2.1.1. Milling material

Colloidal silica (Ludox TM-50, Sigma-Aldrich) was used as model system for agglomeration experiments. Ludox TM-50 is an aqueous dispersion of silica particles with a primary particle size of around 30 nm diameter. The original suspension has a pH value of 8.84 and a solid concentration of 50 wt.%. The experiments have been carried out with a 5 wt.% Ludox suspension. Therefore, the Ludox was diluted in aqueous KOH solution with the same pH value as the original suspension.

The materials used in the milling experiments along with their initial particle sizes are summarized in Table 1.

#### 2.1.2. Solvents

Ethanol (96% denatured with 1% MEK, VWR, Germany) and distilled water were used as dispersants.

#### 2.1.3. Grinding media

Wear resistant, commercially available yttrium-stabilized zirconia ( $ZrO_2$ ) milling beads in the size range of 0.4–0.63 mm (TOSOH, Japan) were used in the milling and agglomeration experiments. According to the manufacturer the grinding media have a density of 6065 kg/m<sup>3</sup> and a chemical composition of 95%  $ZrO_2$  and 5%  $Y_2O_3$ .

### 2.2. Experimental set-up

All milling experiments in aqueous suspensions were carried out in a six disc stirred media mill with a content of 0.95 l. The suspension flows axially through the mill and a sieving cartridge with gaps of 100  $\mu$ m prevents milling beads from leaving the grinding chamber. The grinding chamber is lined for wear protection reasons with ceramic walls (SiSiC) and the stirrer is equipped with discs of polyurethane (PU). The experimental set-up provides a circuit mode comminution of the product. The suspension is pumped with a hose pump from the grinding chamber into a stirred vessel, where samples can be taken and stabilizers added. From the vessel the suspension flows back into the mill.

The commercial laboratory mill LabStar LS 1 (Netzsch, Germany) was used for the milling experiments in ethanol. A schematic diagram of the milling chamber is shown in Fig. 1. The mill has an explosion-

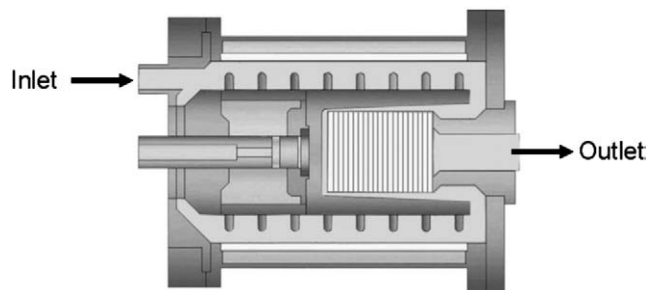


Fig. 1. Schematic diagram of the stirred media mill LabStar LS 1.

proof design and is equipped with a centrifugal separating system for the grinding media. This allows the use of small milling beads down to 0.1 mm. The milling chamber with a volume of 0.68 l as well as the stirrer is lined with  $ZrO_2$ . The experimental set-up for this mill corresponds to the apparatus described above. Both grinding chambers are equipped with a double wall for cooling, which is connected to an internal cooling water system.

### 2.3. Sample characterization

#### 2.3.1. Dynamic Light Scattering (DLS)

The particle size distributions of the milled samples were obtained by measuring the intensity fluctuations of the scattered light of a 3 mW semiconductor laser with a wavelength of 780 nm using the Honeywell Microtrac Ultrafine Particle Analyzer (UPA).

#### 2.3.2. Specific surface area (BET)

BET (Brunauer–Emmett–Teller) measurements to determine the specific surface area of the particles were carried out on a Quantachrome NOVA 2000 gas sorption analyzer. The samples were degassed for 12 h at 150 °C under vacuum to remove adsorbed solvent molecules. The specific surface area was determined using a 7-point method with nitrogen as adsorption gas.

#### 2.3.3. X-ray Diffraction (XRD)

The XRD data was collected using a Siemens D 5000 powder diffractometer with graphite secondary monochromator using  $Cu K_{\alpha}$  radiation ( $\lambda = 0.15406$  nm). The XRD patterns of the samples were recorded with a step width of 0.02° and a counting time of 3.5 s/step. A divergence slit and an anti-scatter slit of 0.5° as well as a detector slit of 0.2 mm were used. The samples were measured in a  $2\theta$  range from  $20^{\circ} \leq 2\theta \leq 80^{\circ}$ .

#### 2.3.4. Scanning Electron Microscopy (SEM)

SEM images were obtained using a Carl Zeiss SMT Gemini Ultra 55 with EDX-detector from Thermo Electron. The concentrated suspension was diluted and dispersed by sonification before spreading it on a cleaned Si-Wafer via spin-coating. The prepared wafer was dried under dust free conditions.

## 3. Results and discussion

### 3.1. Distinction between apparent and true grinding limit

The particle size distribution of a milled suspension is often measured by laser diffraction and in the case of smaller particles ( $<1 \mu$ m) by Dynamic Light Scattering (DLS). In most grinding experiments it is observed that after a certain milling time no further decrease of the particle size occurs and a plateau in particle size is reached.

Fig. 2 illustrates the development of the particle size of quartz particles milled in ethanol without any additive as stabilizer. By comparing the particle sizes from DLS measurements with the primary

Table 1  
Particle size parameters of the inserted materials (measured with laser diffraction).

Material	Trade name	Manufacturer/supplier	$x_{10,3}$	$x_{50,3}$	$x_{90,3}$
SiO <sub>2</sub>	Mikrosil LS 500	Westdeutsche Quarzwerke Dr. Müller GmbH	2.3 $\mu$ m	5.2 $\mu$ m	11.0 $\mu$ m
SiO <sub>2</sub>	CT 1200 SG	Carl Roth GmbH & Co. KG	3.4 $\mu$ m	14.3 $\mu$ m	39.1 $\mu$ m
Al <sub>2</sub> O <sub>3</sub>		Almatis	1.2 $\mu$ m	2.4 $\mu$ m	4.4 $\mu$ m
CaCO <sub>3</sub>		Carl Roth GmbH & Co. KG	0.8 $\mu$ m	7.0 $\mu$ m	13.4 $\mu$ m
SnO <sub>2</sub>		Merck GmbH	0.2 $\mu$ m	1.6 $\mu$ m	5.2 $\mu$ m
ZrO <sub>2</sub>		Sigma-Aldrich	1.0 $\mu$ m	1.8 $\mu$ m	3.3 $\mu$ m

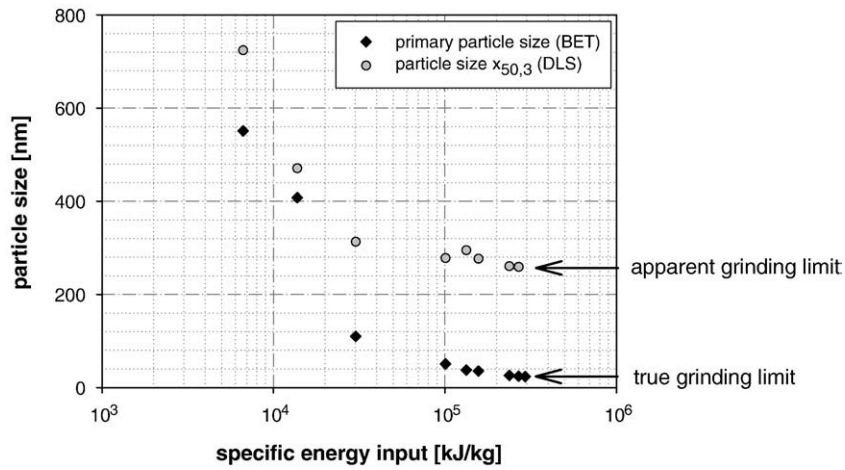


Fig. 2. Distinction between apparent and true grinding limit.

particle sizes determined by the nitrogen adsorption technique, it can be observed that the primary particle sizes are much smaller than those measured by the scattering method. This indicates that the particles have formed agglomerates caused by unstable suspension conditions which cannot be detected by BET. Micropore analysis of the feed material and the final powder at low relative pressures were accomplished to exclude the existence of micropores in the materials which can distort the measured particle size. In Fig. 3 a SEM image of the ground quartz particles is presented. The primary particles with sizes in the nanometer range are agglomerated to structures with a mean diameter between 200 and 400 nm.

The observed plateau in particle size is defined as the apparent grinding limit which is mainly influenced by the stability of the suspension. As can be seen in Fig. 2 the development of the primary particle size also reaches a constant value which is defined as true or real grinding limit. This true grinding limit is the minimal achievable particle size in grinding experiments and can be reached under stable milling conditions where the particle size is not influenced by an agglomeration process but only through real breakage of particles. In the following the influencing parameters on the apparent and true grinding limit will be presented.

3.2. Influencing parameters on the apparent grinding limit

The separation of the competing mechanisms which determine the apparent grinding limit by the following experiments enables a closer

examination of the single process of agglomeration. Besides different stability conditions the influence of the stirrer tip speed on the agglomeration behavior under real milling conditions is presented in the following.

Fig. 4 shows the results of agglomeration experiments carried out with a 5 wt.% aqueous Ludox suspension with different concentrations of KNO<sub>3</sub> and a stirrer tip speed of 4 m/s. Samples were taken directly from the suspension outlet of the mill and were immediately diluted in order to avoid further agglomeration. The volume weighted particle size distribution was measured directly by DLS. As can be seen in Fig. 4 the particle sizes for all salt concentrations increase with milling time until a plateau is reached. It appears that the steady state between agglomeration and deagglomeration occurs in a size range between 200 nm and 400 nm. The kinetics as well as the height of the plateau however depends on the salt concentration in the suspension. For higher salt contents the suspension is more unstable due to compression of the electrostatic double layer [16].

In Fig. 5 the influence of the stirrer tip speed on the agglomeration behavior is shown. A 5 wt.% Ludox suspension with a constant salt concentration of 0.6 M KNO<sub>3</sub> is stressed in the mill with a tip speed of 4 m/s and 8 m/s. In comparison the development of the agglomerate size under perikinetic conditions, where only Brownian motion leads to a collision between the particles, is illustrated. It can be observed that under additional shear stressing of the suspension the kinetics of agglomeration is much faster than that of the perikinetic agglomeration. Furthermore the final particle size in the steady state regime is

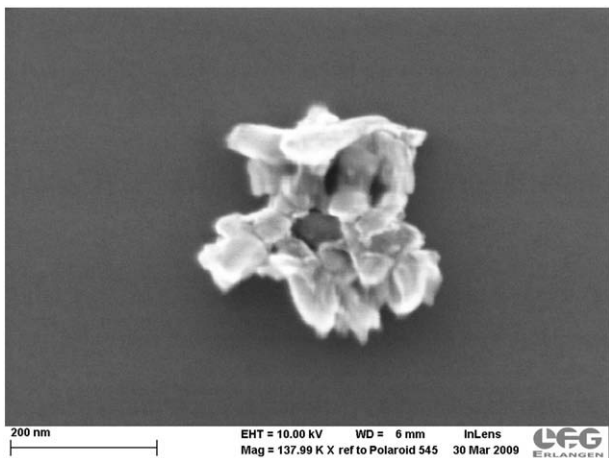


Fig. 3. SEM picture of quartz particles after grinding for 50 h.

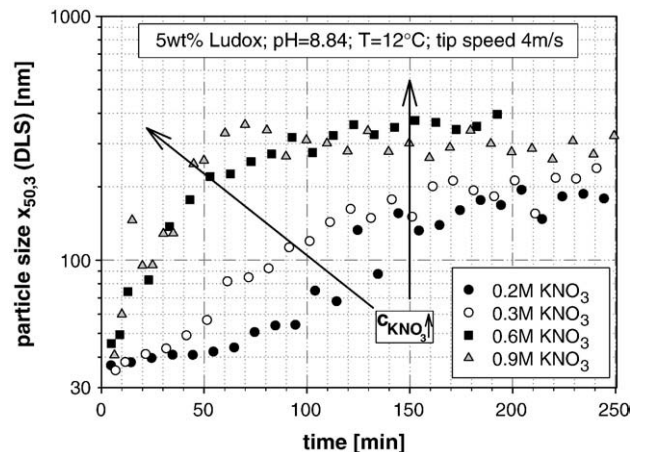


Fig. 4. Influence of different salt concentrations on the agglomeration under milling conditions.



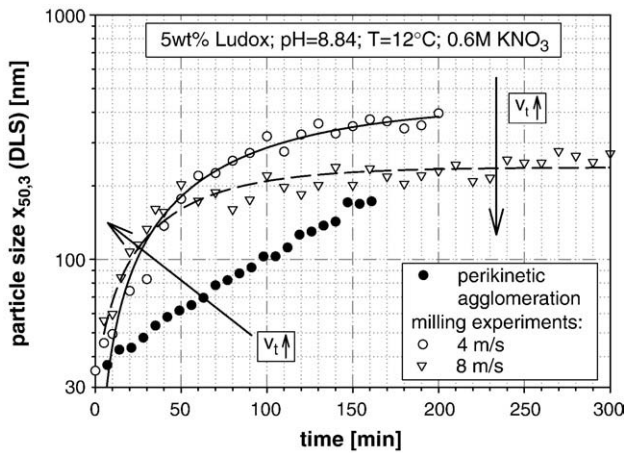


Fig. 5. Influence of the tip speed on the agglomeration under milling conditions compared with perikinetic agglomeration.

smaller with increasing stirrer tip speed. An enhanced rotational speed of the stirrer leads to higher shear forces in the milling chamber. This may cause an increased deagglomeration rate and results in smaller agglomerate sizes. Additionally Sommer [17] found by small angle neutron scattering (SANS) experiments that the fractal dimension of sheared agglomerates increases with higher shear rates. In other words, agglomerates under high shear conditions seem to be more densified, which also results in smaller equivalent diameters measured by DLS. Such densification of agglomerates after applying shear forces has been reported previously [18,19].

To investigate the influence of agglomeration and deagglomeration on the final particle size in a real comminution process, grinding experiments with the  $\text{SiO}_2$  powder Mikrosil LS500 were carried out under the same stability and milling conditions as the presented agglomeration experiments above (see Fig. 6). Comparing the results of the agglomeration experiment with the grinding experiment with a tip speed of 8 m/s and a salt concentration of 0.6 M  $\text{KNO}_3$ , it can be observed that the plateau is nearly at the same particle size. The slightly larger particle sizes in the grinding experiments may be

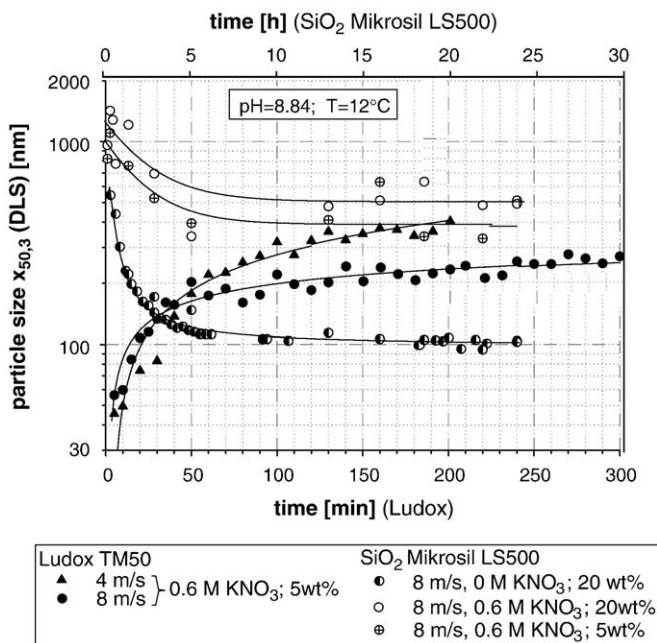


Fig. 6. Evolution of the particle size of agglomerated Ludox and milled Mikrosil particles under same milling conditions.

caused by the higher amount of milling bead attrition and other impurities due to longer stressing times compared to those in the agglomeration experiments leading to a more unstable suspension. The comparison of pure agglomeration experiments with grinding experiments under unstable conditions makes clear that the agglomeration of particles is the main influencing mechanism on the apparent grinding limit. With an increasing solid and salt content the equilibrium particle size is shifted to larger values, which can be explained by a higher agglomeration rate.

### 3.3. Breakage behavior and the true grinding limit of different materials

Through improving the suspension stability the agglomeration of particles can be reduced or in some cases completely avoided. The particle size in the milled suspension is then only determined by real particle breakage. This can be described by the evolution of the primary particle size with milling time. Under the assumption that particle breakage occurs at the grain boundaries, i.e. the weakest points in a polycrystalline material, the development of the crystallite size can be used to explain the breakage process. Fig. 7 illustrates the X-ray diffraction patterns of zirconia particles of the initial state and after 50 h of stressing in a stirred media mill. A loss in crystallinity occurs with milling time. The peaks of the milled zirconia are significantly broadened which may be caused by either decreasing crystallite size and/or enhanced strain in the lattice of the domains.

The crystallite sizes and the microstrains of the milled powders were determined from the X-ray patterns with a Rietveld refinement [20] using the commercial software package TOPAS (Bruker AXS). For modelling microstructural effects TOPAS is supported by the Double-Voigt Approach (e.g. Balzar [21]). The possibility for a separate size-strain analysis is given by the effect that size broadening is angle independent, whereas strain broadening depends on the diffraction angle [21].

In Fig. 8 the evolution of the primary particle size, the crystallite size and the strain of zirconia particles over the specific energy input is shown. It can be observed that the crystallite size decreases until a plateau at a critical crystallite size (volume weighted) of about 4.5 nm and a primary particle size (area weighted) of approximately 4 nm are achieved. Comparing the crystallite sizes with the primary particle sizes one can assert that above a certain energy input the initially polycrystalline zirconia particles become monocrystalline. From this point on particle breakage can only occur if a crystallite size reduction preceded. The strain inside the crystallites increases at the beginning of the milling experiment until a maximal value is reached and afterwards decline to nearly zero. Due to the intensive stressing of the particles between the milling beads lattice imperfections are generated, enhancing the total amount of elastically stored energy

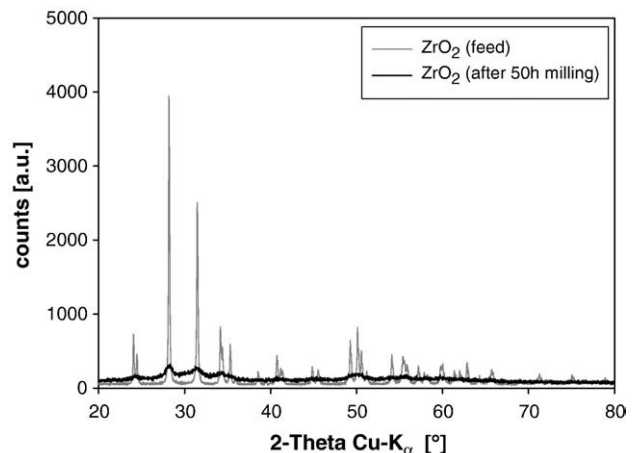


Fig. 7. Diffraction patterns of zirconia before and after 50 h milling.

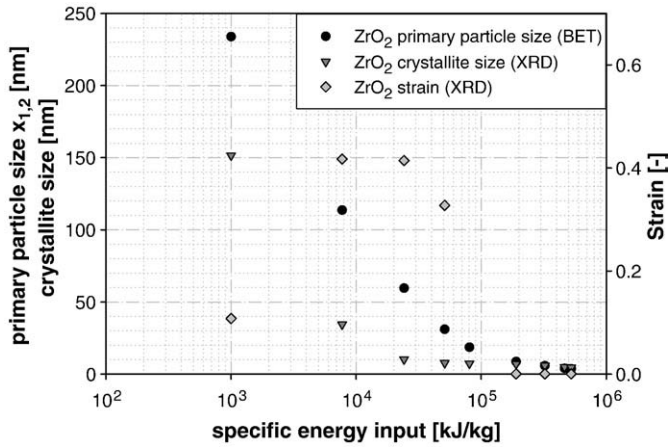


Fig. 8. Evolution of primary particle size, crystallite size and strain of zirconia with specific energy input.

in a crystallite. After reaching a critical crystallite size it is assumed that the domains become so small that it is no longer possible for the lattice to store defects [22]. As a result of this mechanism the strain decreases to a minimum. In Fig. 8 the disappearance of lattice strain corresponds to the point where no further reduction of the crystallite size occurs and the true grinding limit is reached. It is supposed that below a certain particle size the transferred stress intensity from the milling beads is no longer sufficient to achieve a brittle fracture with a single impact. Hence, further breakage can only occur if the elastically stored energy provided from lattice imperfections and external mechanical impact is sufficient to fulfill the integral energy balance and enable a fracture to traverse the entire particle [23]. This behavior of a fatigue fracture explains the reduced breakage kinetics in the nanometer range. Accordingly, it can be concluded that the generation of defects enables the breakage in the nanometer range whereas their absence below a critical size determines the grinding limit.

The kinetics of particle breakage as well as the grinding limit depends on a multitude of influencing variables. These influencing variables can be separated into three groups:

- Material parameters (material properties of the milling powder, properties of the solvent, stability conditions)
- Process parameters (rotational speed of the stirrer, milling bead size and material, etc.)
- Machine parameters (design of the mill, kind of stressing, etc.).

We have investigated the influence of different materials on the breakage behavior of particles in the nanometer range and their grinding limit. For this study five different materials ( $ZrO_2$ ,  $Al_2O_3$ ,  $SnO_2$ ,  $SiO_2$  and  $CaCO_3$ ) were stressed in a stirred media mill. The milling experiments were carried out under the same following conditions: milling bead size 0.4–0.5 mm, filling ratio of the grinding chamber with milling beads 80% and stirred tip speed 8 m/s. Whereas particles of  $SnO_2$  and  $CaCO_3$  were milled in water, the other materials were milled in ethanol. However, as ethanol and water do not vary much in their viscosity, the influence of the different solvents can be neglected.

After stressing the particles for about 50 h, most of the materials have reached their grinding limit. The continually decreasing final mean crystallite sizes of some materials may be caused by a crystallite size distribution which gets narrower as large crystallites are still breaking while the smaller ones have already reached their grinding limit. Additionally an amorphization of the particle surface due to intensive mechanical stressing can also lead to slightly smaller crystallite sizes without implying a breakage of the crystallites.

Fig. 9 illustrates that each material shows a different breakage behavior expressed in different breakage kinetics as well as in a

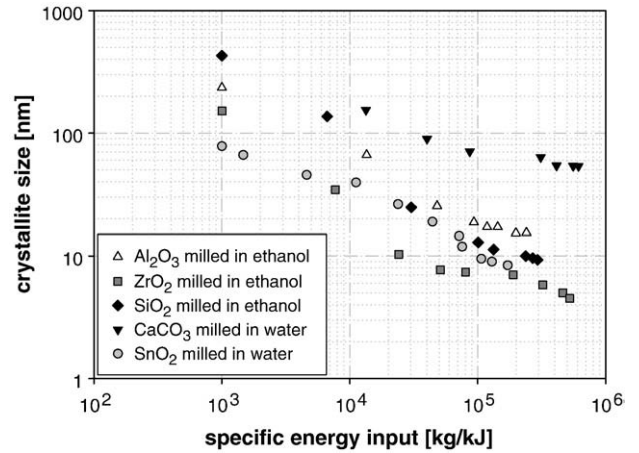


Fig. 9. Development of crystallite sizes for different materials with specific energy input.

different grinding limit. In general the kinetics of crystallite breakage can be approximated by a power function:

$$x = a \cdot E_m^{-b} \quad (1)$$

where  $E_m$  is the mass specific energy input and  $a$  and  $b$  are parameters depending on material and process properties.

For ductile materials like calcium carbonate the smallest crystallite size reached in the milling experiment under the chosen conditions was about 55 nm whereas for very brittle materials like zirconia a grinding limit of less than 5 nm was observed. Ductile materials respond to mechanical stressing with distinct plastic deformation whereas in brittle materials the applied energy is mainly used for particle fracture. We have to point out that the reached grinding limits are not fixed values. It should become clear that under different milling conditions, for example by changing the rotational speed of the stirrer other stress intensities and therefore different values of the true grinding limit might be achieved.

A direct correlation of the minimal crystallite sizes with material properties is difficult for the time being, because of a superposition of material and process parameters both influencing the breakage behavior. To illustrate this problem the minimal crystallite sizes are shown for each material in relation to their Young's moduli in Fig. 10.

The Young's modulus is a measure for the resistance of a material against elastic deformation. If the Young's modulus is small, the material uses much of the inserted energy for deformation so that only a small amount is available for breakage. This might be an explanation for the large grinding limit of calcium carbonate in comparison with

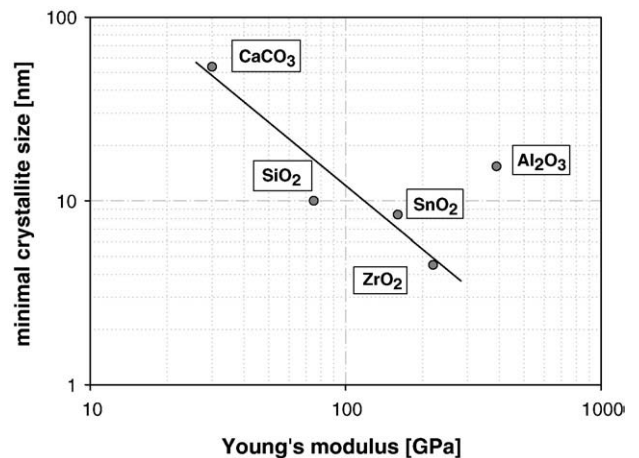


Fig. 10. Influence of Young's modulus on the grinding limit.

zirconia or tin oxide. Becker et al. [24] observed that the portion of energy which can be transferred from the grinding media to the product particles during the stressing event strongly depends on the ratio of Young's moduli of the product particles and the grinding media caused by a deformation of milling beads. In the case of fused alumina particles compared with calcium carbonate particles both stressed with yttrium-stabilized zirconium oxide milling beads the transferred stress intensity is more than 50% lower for the alumina particles. Thus the total energy might not be sufficient to reach further crystallite size reduction as explained above and a larger final crystallite size of alumina is achieved than expected due to its large Young's modulus. To correlate the material properties with the grinding limit and the breakage kinetics a separation of process and material parameters is necessary. In addition, the Young's modulus is probably not the only influencing material parameter to describe the breakage behavior of particles. As Meier et al. [25] have shown for larger pharmaceutical particles in single particle impact comminution experiments, the breakage behavior mainly depends on the brittleness index which is defined as ratio of hardness to fracture toughness. Moreover, it is unclear for the time being how the material properties are changing with particle size especially in the nanometer range and degree of distortion. Further investigations on this topic are in progress and will be presented in forthcoming papers.

#### 4. Conclusions

The agglomeration of particles in a comminution process is the main influencing mechanism on the apparent grinding limit. With agglomeration experiments inside a stirred media mill under different stability conditions it was shown, that the final agglomerate size depends on the suspension stability as well as on the available shear forces in the milling chamber. Compared with real grinding experiments under the same stability conditions nearly the same steady state in particle size is reached. The particle size in an agglomerate-free suspension is only determined by actual particle breakage. A grinding limit is identified in long term experiments for different materials and could be characterized by the crystallite size measured by X-ray diffraction. This true grinding limit is the minimal achievable particle size under the applied milling conditions. It is assumed that the grinding limit is reached due to an insufficient amount of elastically stored energy in the particles. During the grinding process lattice imperfections are generated which enhance the amount of stored energy and lead together with the transferred energy from the milling beads to further particle breakage. The procedure of generating defects until the available elastic energy is large enough to fulfill the integral energy balance reduces the breakage kinetics in the nanometer range. The grinding limit is reached when the crystallites become so small that no defects can be stored in the lattice anymore. The total available energy at this critical crystallite size is insufficient and could not be increased by further milling. Accordingly, the generation of defects enables nanogrinding by increasing the elastically stored energy, but determines with its disappearance below a critical size concurrently the overall limit of grinding.

The kinetics of particle breakage and the true grinding limit depend on material properties as well as on process parameters influencing the stress intensity. A correlation between those parameters and the particle size will be determined by a separation of the material function and the machine function in future works.

#### Acknowledgements

This work was financially supported by the German Research Council (DFG) and the International Fine Particle Research Institute (IFPRI). We gratefully acknowledge Prof. Neubauer and Christoph Hesse of the Institute of Mineralogy for their support in analyzing the XRD patterns. Additionally, we thank the NETZSCH-Feinmahltechnik GmbH for providing the laboratory mill "LabStar".

#### References

- [1] F. Stenger, S. Mende, J. Schwedes, W. Peukert, Nanomilling in stirred media mills, *Chemical Engineering Science* 60 (16) (2005) 4557–4565.
- [2] F. Stenger, S. Mende, J. Schwedes, W. Peukert, The influence of suspension properties on the grinding behavior of alumina particles in the submicron size range in stirred media mills, *Powder Technology* 156 (2–3) (2005) 103–110.
- [3] M. Sommer, F. Stenger, W. Peukert, N.J. Wagner, Agglomeration and breakage of nanoparticles in stirred media mills – a comparison of different methods and models, *Chemical Engineering Science* 61 (1) (2006) 135–148.
- [4] W. Peukert, H.-C. Schwarzer, F. Stenger, Control of aggregation in production and handling of nanoparticles, *Chemical Engineering and Processing* 44 (2) (2004) 245–252.
- [5] C. Suryanarayana, Mechanical alloying and milling, *Progress in Materials Science* 46 (1–2) (2000) 1–184.
- [6] G. Scholz, I. Doerfel, D. Heidemann, M. Feist, R. Stoesser, Nanocrystalline CaF<sub>2</sub> particles obtained by high-energy ball milling, *Journal of Solid State Chemistry* 179 (4) (2006) 1119–1128.
- [7] A. Revesz, T. Ungar, A. Borbely, J. Lendvai, Dislocations and grain size in ball-milled iron powder, *Nanostructured Materials* 7 (7) (1996) 779–788.
- [8] P. Pourghahramani, E. Forsberg, Microstructure characterization of mechanically activated hematite using XRD line broadening, *International Journal of Mineral Processing* 79 (2) (2006) 106–119.
- [9] P. Pourghahramani, E. Altin, M.R. Mallebakam, W. Peukert, E. Forsberg, Microstructural characterization of hematite during wet and dry millings using Rietveld and XRD line profile analyses, *Powder Technology* 186 (1) (2008) 9–21.
- [10] C.C. Koch, Synthesis of nanostructured materials by mechanical milling: problems and opportunities, *Nanostructured Materials* 9 (1–8) (1997) 13–22.
- [11] G.R. Karagedov, N.Z. Lyakhov, Mechanochemical grinding of inorganic oxides, *KONA* 21 (2003) 76–87.
- [12] V.V. Boldyrev, S.V. Pavlov, E.L. Goldberg, Interrelation between fine grinding and mechanical activation, *International Journal of Mineral Processing* 44–45 (1996) 181–185.
- [13] H. Cho, M.A. Waters, R. Hogg, Investigation of the grind limit in stirred-media milling, *International Journal of Mineral Processing* 44–45 (1996) 607–615.
- [14] J. Eckert, J.C. Holzer, C.E. Krill, W.L. Johnson, Structural and thermodynamic properties of nanocrystalline fcc. metals prepared by mechanical attrition, *Journal of Materials Research* 7 (7) (1992) 1751–1761.
- [15] K. Schönert, K. Steier, Die Grenze der Zerkleinerung bei kleinen Korngrößen, *Chemie Ingenieur Technik* 43 (3) (1971) 773–777.
- [16] J. Israelachvili, *Intermolecular and Surface Forces*, Academic Press, London, 1991.
- [17] M. Sommer, *Mechanical Production of Nanoparticles in Stirred Media Mills*, PhD thesis, Erlangen-Nuremberg 2007.
- [18] F.E. Torres, W.B. Russel, W.R. Schowalter, Floc structure and growth kinetics for rapid shear coagulation of polystyrene colloids, *Journal of Colloid and Interface Science* 142 (2) (1991) 554–574.
- [19] P.D.A. Mills, J.W. Goodwin, B.W. Grover, Shear field modification of strongly flocculated suspensions aggregate morphology, *Colloid and Polymer Science* 269 (1991) 949–963.
- [20] H.M. Rietveld, Profile refinement method for nuclear and magnetic structures, *Journal of Applied Crystallography* 2 (2) (1969) 65–71.
- [21] D. Balzar, Voigt function model in diffraction-line broadening analysis, *International Union of Crystallography Monographs on Crystallography* 10 (1999) 94–126 (Defect and Microstructure Analysis by Diffraction).
- [22] V.G. Gryaznov, I.A. Polonsky, A.E. Romanov, L.I. Trusov, Size effects of dislocation stability in nanocrystals, *Physical Review B* 44 (1) (1991) 42.
- [23] S. Bernotat, K. Schönert, Size reduction, *Ullmann's Encyclopedia of Industrial Chemistry* 7th ed., 2007, release.
- [24] M. Becker, A. Kwade, J. Schwedes, Stress intensity in stirred media mills and its effect on specific energy requirement, *International Journal of Mineral Processing* 61 (3) (2001) 189–208.
- [25] M. Meier, E. John, D. Wieckhusen, W. Wirth, W. Peukert, Influence of mechanical properties on impact fracture: prediction of the milling behaviour of pharmaceutical powders by nanoindentation, *Powder Technology* 188 (3) (2009) 301–313.